

Observation of magnetic order in $\text{La}_{1.9}\text{Sr}_{0.1}\text{CuO}_4$ from two-magnon Raman scattering

Y. Lin, J. Sichelschmidt, J. E. Eldridge

Department of Physics and Astronomy, University of British Columbia, Vancouver, B.C. V6T 1Z1, Canada

T. Wahlbrink

Fachbereich Physik der Universität Osnabrück, 49069 Osnabrück, Germany

S.-W. Cheong

Department of physics, Rutgers University, Piscataway, New Jersey 08855

Bell Laboratories, Lucent Technologies, Murray Hill, New Jersey 07974

(October 12, 2018)

We report two-magnon Raman scattering from $\text{La}_{1.9}\text{Sr}_{0.1}\text{CuO}_4$, which has a suppressed $T_c=12$ K, as the temperature is lowered below 37 K and an ordered spin phase is formed. The two-magnon Raman intensity increases with decreasing temperature. The magnetic scattering in $\text{La}_{1.9}\text{Sr}_{0.1}\text{CuO}_4$ is totally different from that reported in the parent compound La_2CuO_4 . We analyze the line shape of the two-magnon scattering within the traditional Loudon-Fleury theory and find the superexchange constant $J=1052$ cm^{-1} . The calculation of the frequency moment suggests that the quantum fluctuations are very weak in the system. The room temperature Raman scattering from La_2CuO_4 is also measured. Strong features appear in the one-phonon spectrum at the frequencies of the longitudinal optical (LO) infrared modes which we suggest become Raman active through a Fröhlich-interaction.

PACS numbers: 74.25.Ha, 78.30.-j, 72.10.Di, 74.72.-h

I. INTRODUCTION

One of the most important questions in the study of the cuprate superconductors is the understanding of the phase diagram of these materials, especially the interplay between magnetism and superconductivity (SC). La_2CuO_4 , which is the parent compound of the “214” high- T_c cuprate superconductors $\text{La}_{2-x}\text{Sr}_x\text{CuO}_4$ and $\text{La}_{2-x}\text{Ba}_x\text{CuO}_4$ with the simple structure of single CuO_2 layers, is an insulating antiferromagnet with a transition temperature T_N around 300 K and spin $s=1/2$, localized on Cu atoms in the CuO_2 planes. With increasing dopant x above 0.06, $\text{La}_{2-x}\text{Sr}_x(\text{Ba})_x\text{CuO}_4$ become superconducting. However, at x around 0.11 in $\text{La}_{2-x}\text{Sr}_x\text{CuO}_4$ and x around 0.125 in $\text{La}_{2-x}\text{Ba}_x\text{CuO}_4$, the superconductivity is suppressed and magnetic ordering reemerges.^{1–10}

In the $\text{La}_{2-x}\text{Ba}_x\text{CuO}_4$ (x around 0.12), a structural phase transition, from the low temperature orthorhombic phase (LTO) to the low temperature tetragonal phase (LTT), has been observed at $T=70$ K.^{2,11} Below 36 K, the magnetic ordering was observed by μSR and NMR measurements.^{3,6,9} In the $\text{La}_{2-x}\text{Sr}_x\text{CuO}_4$ ($x=0.12$), Moodenbaugh *et al*¹² observed an incomplete phase transformation (approximately 10 %) below 80 K from the LTO phase to the LTT phase, using high-resolution synchrotron x-ray powder diffraction. The LTT phase was also indicated by electron diffraction and ultrasonic measurements.^{10,11,13} There have been several reports of magnetic ordering in $\text{La}_{2-x}\text{Sr}_x\text{CuO}_4$ (x around 0.11) at low temperatures.^{4,6–10} The ³⁹La and ^{63/65}Cu-NMR showed an antiferromagnetic ordering below 32 K⁹ and the Cu-spin moments were found to be in

the CuO_2 plane perpendicular to the c -axis.^{7,9} Most recently, Suzuki *et al* observed a long-range magnetic order developing below 45 K in $\text{La}_{1.88}\text{Sr}_{0.12}\text{CuO}_4$.¹⁰ Recently, a stripe mechanism^{14–18} has been proposed to explain the suppression of the superconductivity. In the low temperature stripe phase, the doped holes are concentrated in domain walls separating antiferromagnetic antiphase domains. Stripes becomes pinned or immobilized only in the LTT phase but not in the LTO phase.

Motivated by a successful observation of the spin-ordered phase at low temperatures in $\text{La}_{1.67}\text{Sr}_{0.33}\text{NiO}_4$ by Raman scattering,^{19,20} we performed a Raman measurement on the magnetic scattering at low temperatures in $\text{La}_{2-x}\text{Sr}_x\text{CuO}_4$ crystals and found strong two-magnon scattering from a $\text{La}_{1.9}\text{Sr}_{0.1}\text{CuO}_4$ crystal. To distinguish the magnetic Raman scattering in $\text{La}_{1.9}\text{Sr}_{0.1}\text{CuO}_4$ from that in the parent compound La_2CuO_4 under the same laser excitation, we also performed a Raman measurement on La_2CuO_4 . Two-magnon Raman scattering has been intensively studied in the parent compound La_2CuO_4 .^{21–24} A very broad peak around 3200 cm^{-1} and a long tail at higher energy have been reported. Many theories have been developed to explain the broad Raman line shape.^{24–29} Singh *et al*.²⁴ evaluated the first three frequency moments and cumulants of the line shape, which provided a quantitative, parameter-free check on the theoretical prediction for the effect of quantum fluctuations (QF) in the system.²⁴ The Fleury-Loudon theory³⁰ in the spin wave formalism was examined again by several groups^{25–29} Using these theories the authors obtained the superexchange constant $J=1030$ cm^{-1} , which is in good agreement with the value obtained from neutron scat-

tering measurement.^{31,32} However the total line shape given by the theories is still in rather poor agreement with the experimental line shape. Recently, Chubukov, Frenkel and Morr^{26–28} published a triple resonance theory, based on the resonance Raman scattering theory in the spin density wave formalism. The theory successfully explained the dependence of the two-magnon peak intensity on the incoming photon frequency, which was one of the key experimental puzzles.^{33,34}

The Raman phonon spectrum of La_2CuO_4 is also strongly dependent on the frequency of the incoming photon. It is dominated by very strong two-phonon scattering when the incoming photon is close to the charge-transfer gap 2Δ (2.0 eV),^{33,35,36} while the two-magnon scattering vanishes there^{33,36} and instead has a maximum when the photon has energy equal to $2\Delta+3J$.^{26,27,33,34} Some single phonon scattering peaks have been thought to originate from Brillouin zone boundary phonons.^{36,37} Some Raman-forbidden phonons have also been observed.^{36–38} Heyen, Kircher and Cardona³⁹ carefully examined the Raman scattering from $\text{YBa}_2\text{Cu}_3\text{O}_6$ using different lasers. They explained the appearance of four usually-infrared-active-only LO phonons in the Raman spectrum as a result of a Fröhlich-interaction. They also pointed out that the unexpected peaks found in La_2CuO_4 were Fröhlich-interaction induced LO phonons.

In this paper, a much narrower two-magnon Raman peak around 3400 cm^{-1} is observed below 37 K from single crystal $\text{La}_{2-x}\text{Sr}_x\text{CuO}_4$ ($x=0.1$), which has a suppressed T_c of 12 K. The magnetic Raman intensity increases with decreasing temperature and persists at 2 K. The Raman line shape is fitted within the Loudon-Fleury Raman theory and the superexchange constant J was obtained. For La_2CuO_4 , strong single-phonon scattering from the whole Brillouin zone is reported. Seven intense usually-infrared-active LO phonons are observed, which may become Raman active via the Fröhlich interaction.

II. EXPERIMENT

$\text{La}_{1.9}\text{Sr}_{0.1}\text{CuO}_4$ and one of the La_2CuO_4 crystals were prepared using spontaneous crystallization from a CuO flux.⁴⁰ The other La_2CuO_4 crystal was prepared at Bell laboratories. After annealing in Ar gas, the crystal has a $T_N=315\text{ K}$, close to the accepted value $T_N=320\text{ K}$ for the stoichiometric compound. The Raman measurements were made on the interior surface of the crystals exposed by mechanical fracture and repeated on the polished surfaces from both sides of the crystals.

The Raman measurements were performed with a Bruker RFS 100 Fourier Raman spectrometer, which op-

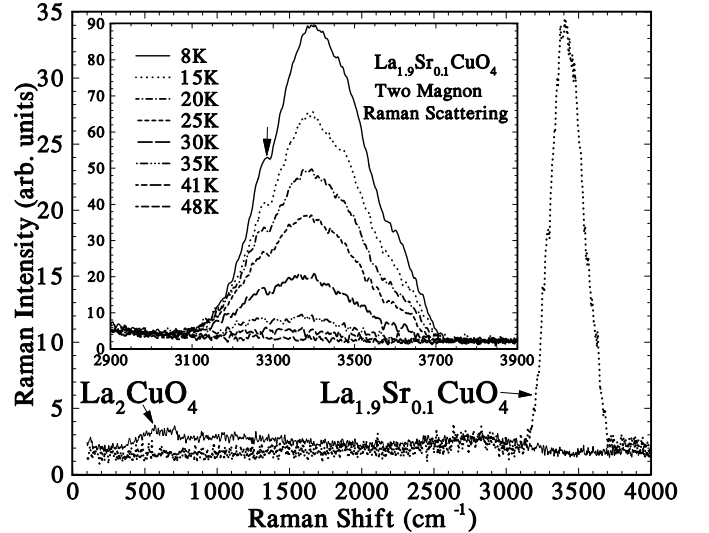


FIG. 1. Raman spectra of $\text{La}_{1.9}\text{Sr}_{0.1}\text{CuO}_4$ at 2 K and La_2CuO_4 at 8 K between 100 and 4000 cm^{-1} with a laser power of 5 mW and an average of 1,200 scans. The insert shows the temperature dependent two-magnon Raman scattering in $\text{La}_{1.9}\text{Sr}_{0.1}\text{CuO}_4$ between 2900 and 3900 cm^{-1} . The spectra look much narrower than the two-magnon scattering around 3200 cm^{-1} from the parent compound La_2CuO_4 under the excitation of a visible laser, and have a strong temperature-dependence. An arrow indicates another possible peak.

erates with an infrared diode-pumped Nd:YAG laser with wavelength of 1064 nm. Most of the low temperature measurements were taken with an Air-Products Heli-Tran refrigerator with a polypropylene vacuum-shroud window. The sample was mounted on the copper disc with APIEZON grease. Two silicon diodes for temperature measurement and control were mounted on the cold finger, with one immediately adjacent to the sample. The laser power was 6 mW at low temperatures. If the laser power was raised above 60 mW, the magnetic Raman scattering was no longer observed. The lowest temperature measurement at 2 K was performed in a Janis refrigerator with the sample completely immersed in superfluid liquid helium. A back-scattering geometry was employed. At low temperatures, the linearly polarized incident beam was focused on the ab plane of the crystal surface. The spectrum was independent of the laser spot location.

III. RESULTS

Fig. 1 shows the Raman spectrum of $\text{La}_{1.9}\text{Sr}_{0.1}\text{CuO}_4$ at 2 K with a very strong and sharp peak centered at 3419 cm^{-1} . This is two-magnon scattering which has been intensively investigated by experiments in La_2CuO_4 and $\text{YBa}_2\text{Cu}_3\text{O}_{6+\delta}$ ^{21–24,34} and theories.^{26,27} For comparison, the spectrum of La_2CuO_4 is also showed in the figure

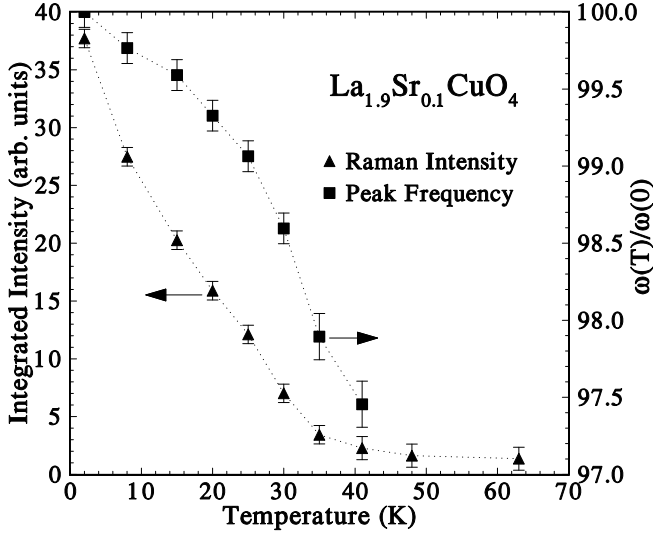


FIG. 2. Two-magnon Raman intensity and peak frequency as a function of temperature. The integrated intensity was obtained from the averaged results both with and without the background scattering. We obtained the peak value by fitting the spectrum to a Gaussian.

under the same conditions. It may be seen that the two-magnon scattering in La_2CuO_4 is not observed with the infrared laser. This is because the laser frequency of $9,394 \text{ cm}^{-1}$ is below the charge transfer gap of $16,100 \text{ cm}^{-1}$ (2.0 eV),³⁶ and so the intensity of two-magnon scattering will be very weak. This dependence has been observed experimentally^{33,34} and explained by the triple resonance theory.^{26–28} The reappearance of the two-magnon scattering in $\text{La}_{1.9}\text{Sr}_{0.1}\text{CuO}_4$ can be explained by the reemergence of the magnetic order at low temperatures in $\text{La}_{2-x}\text{Sr}_x\text{CuO}_4$ with x around 0.11.^{4,6–10} The different behavior of two-magnon Raman scattering with the infrared laser between $\text{La}_{1.9}\text{Sr}_{0.1}\text{CuO}_4$ and La_2CuO_4 indicates that the magnetic structure in $\text{La}_{1.9}\text{Sr}_{0.1}\text{CuO}_4$ is different from that in La_2CuO_4 .

Two-magnon Raman scattering records mainly short wavelength (large k near the Brillouin zone boundary) magnetic excitations. The magnetic interaction in the CuO_2 planes can be described by a Heisenberg Hamiltonian on the two-dimensional square lattice: $H = J \sum_{\langle i,j \rangle} \mathbf{S}_i \cdot \mathbf{S}_j$, where \mathbf{S}_i is the spin-1/2 operator at site i and the summation is over nearest-neighbor Cu pairs. The scattering process involves a photon-stimulated virtual charge-transfer excitation that exchanges two-spins.²⁷ A value of the exchange constant J can be extracted from the Raman scattering. Spin-wave theory^{25,27,29,41} predicts a peak value at $\omega_p = 2.78J_{eff}$. Considering the spin-wave interaction on the magnon, we must apply a relationship $J_{eff} = Z_c J$ with a renormalization factor Z_c which is averaged to be 1.168 from results calculated by the spin wave theory and series expansion estimates.^{25,42,43} We measured $\omega_p = 3419 \text{ cm}^{-1}$.

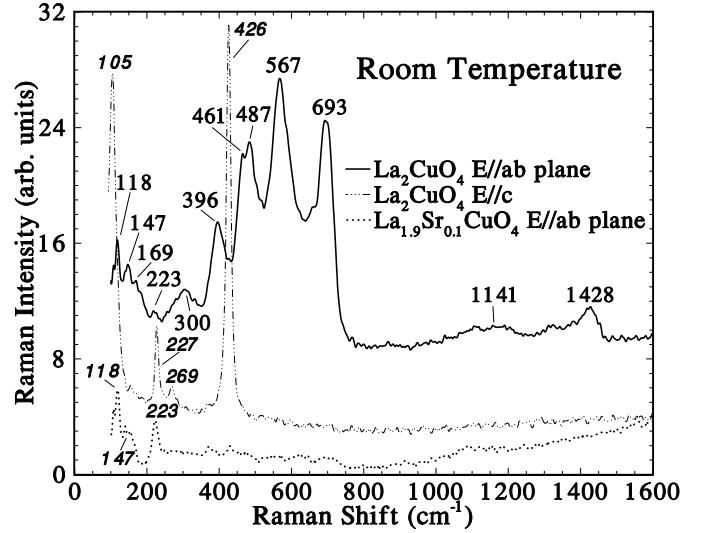


FIG. 3. Raman spectra of La_2CuO_4 and $\text{La}_{1.9}\text{Sr}_{0.1}\text{CuO}_4$ at room temperature between 100 and 1600 cm^{-1} with a laser power of 25 mW and an average of $12,000$ scans.

Thus we get $J = 1052 \text{ cm}^{-1}$. This is in very good agreement with $J = 1042 \text{ cm}^{-1}$ (1500 K) which was used to fit the temperature dependence of the g factor in the electron-paramagnetic resonance (EPR) measurement of $\text{La}_{1.9}\text{Sr}_{0.1}\text{CuO}_4$.⁴⁴

The insert of Fig. 1 shows the two-magnon Raman spectra of $\text{La}_{1.9}\text{Sr}_{0.1}\text{CuO}_4$ between 2900 and 3900 cm^{-1} as a function of temperature. We note from Fig. 1 the following properties of the Raman feature: (i) The two-magnon Raman intensity has a strong temperature dependence. However no appreciable temperature variation of the two-magnon scattering has been observed in La_2CuO_4 for $0 < T < 300 \text{ K}$;^{21,24} (ii) The Raman line (covering 3100 to 3700 cm^{-1}) looks very narrow compared with that from La_2CuO_4 which has a broad Raman feature extending from 2000 to over 7000 cm^{-1} ; (iii) The Raman peak is more symmetric than that in La_2CuO_4 as we will show by calculating the first three cumulants.²⁴

The temperature-dependent integrated Raman intensity, as well as the peak frequency, are plotted in Fig. 2. The intensity decreases with increasing temperature up to 37 K . It is clear that the short-range antiferromagnetic order begins to be established at about 37 K , which is close to the temperature where the magnetic order has been reported by NMR and neutron-scattering for $x = 0.11$ and 0.12 ^{9,10} in $\text{La}_{1-x}\text{Sr}_x\text{CuO}_4$. The magnetic scattering is still seen at 2 K below T_c , which suggests a local coexistence of superconductivity and magnetic ordering as has been seen in other materials.^{16,18,45} It is also shown in Fig. 2 that the peak frequency decreases as the temperature is increased. The frequency is reduced by 2.5% at 37 K , which is very similar to the behavior of the two-magnon peak in the two-dimensional

TABLE I. Frequencies (cm^{-1}) of the observed unexpected Raman peaks in the Raman spectrum compared with the calculated transverse and longitudinal optical (TO and LO, respectively) modes from the infrared (IR) measurements.

Raman "forbidden"	IR (Ref. 49)		IR (Ref. 50)		IR (Ref. 51)	
	ω_{LO}	ω_{TO}	ω_{LO}	ω_{TO}	ω_{LO}	ω_{TO}
169	168	98	183	162		
300	260	168	250	220	300	148
396			390	363	391	359
461	460	229	463	320		
487	461	330			498	234
567	566	480	574	501	535	516
693	692	673	683	671	689	669

antiferromagnet K_2NiF_4 ⁴⁶ where the spin wave theory of two-magnon interaction works very well.⁴¹ The two-dimensional system is unlike three-dimensional compounds which have a stronger temperature dependence of the peak frequency.^{46,47} We should point out that at higher temperatures the $\text{La}_{1.9}\text{Sr}_{0.1}\text{CuO}_4$ crystals have the K_2NiF_4 -type structure.

Fig. 3 shows the polarized room-temperature Raman spectra below 1600 cm^{-1} . Two-phonon scattering in La_2CuO_4 , which is the main feature observed under the excitation of visible lasers, becomes weak here since the infrared laser is far away from the charge-transfer gap. The $E//ab$ single-phonon spectrum, observed here with the infrared laser, is unusual. Firstly, the strong peaks at $693, 567, 487, 461,$ and 396 cm^{-1} are not expected in the Raman spectrum.³⁶⁻³⁸ Secondly, compared with the neutron scattering data, the peak at 693 cm^{-1} has the value of the highest-energy phonon branch with the k vector around $(0.25, 0.25, 0)$,^{36,48} which is in the middle of the Brillouin zone. It is the same for the other strong peaks at $567, 461,$ and 396 cm^{-1} . Normally only zone-center phonons are Raman allowed by the momentum conservation rule. Thirdly, these strong peaks appear very broad, which probably points to contributions from the whole Brillouin zone. Fourthly, these peak frequencies are identical to those of infrared LO phonons as may be seen from Table I.

IV. DISCUSSIONS

We will discuss the following issues in this section: (i) the magnetic order below 37 K in $\text{La}_{1.9}\text{Sr}_{0.1}\text{CuO}_4$. (ii) the line shape of the two-magnon Raman scattering and the theoretical fitting within the Loudon-Fleury theory; (iii) the peak symmetry of the two-magnon Raman spectrum and the quantum-fluctuation effect; (iv) the Fröhlich-interaction induced Raman scattering from normally-Raman-inactive LO phonons in La_2CuO_4 .

The charge and spin stripe phase is a common feature for nickle and manganese oxide analogues of the copper oxides- $\text{La}_{2-x}\text{Sr}_x\text{NiO}_4$ and $\text{La}_{2-x}\text{Sr}_x\text{MnO}_4$.^{52,53} The spin ordering is driven by the charge ordering. Raman scattering from charge and spin ordered stripe phases has been successfully observed in $\text{La}_{1.2}\text{Sr}_{1.3}\text{NiO}_4$ by two research groups.^{19,20} The charge ordering has been observed by electron diffraction in $\text{La}_{2-x}\text{Sr}_x\text{CuO}_4$ ($x=0.115$) below 104 K .¹¹ In $\text{La}_{1.9}\text{Sr}_{0.1}\text{CuO}_4$ we observed a magnetic order below 37 K but we did not observe the phonon changes due to the charge ordering since the phonon scattering is very weak. Although no direct evidence has been obtained from the Raman spectrum, it is still possible that an ordered spin stripe phase is formed below 37 K in $\text{La}_{1.9}\text{Sr}_{0.1}\text{CuO}_4$.

The two-magnon Raman spectrum of the Heisenberg model can be discussed within traditional Loudon-Fleury Raman theory.^{27,29,30} An effective Hamiltonian for the interaction of light with spin degrees of freedom is given by:

$$H_{LF} = \alpha \sum_{\langle i,j \rangle} (\mathbf{e}_i \cdot \mathbf{R}_{ij})(\mathbf{e}_s \cdot \mathbf{R}_{ij}) \mathbf{S}_i \cdot \mathbf{S}_j \quad (1)$$

where \mathbf{e}_i and \mathbf{e}_s are the polarization vectors of the incident and scattered light, α is the coupling constant, and \mathbf{R} is a unit vector connecting two nearest-neighbor sites i and j .

Chubukov and Frenkel carried out a spin-wave expansion of the profile around its peak position by keeping S large and evaluated the results at $S=1/2$. They obtained a formula for the Raman intensity for a B_{1g} mode²⁷ (From equation (A9) of Ref. 27. An error in the denominator of the formula has been corrected):

$$R_{B_{1g}} \propto \frac{S^2 \sqrt{1 - \varpi^2} \ln(1 - \varpi^2)}{\ln^2(1 - \varpi^2) + \pi^2(1 - (S + 1)\sqrt{1 - \varpi^2})^2} \quad (2)$$

where $\varpi = \omega / (8Z_c JS)$. In Fig. 4 we fitted our experimental data with the above formula by a least-square method. We set S as a parameter and found $S=0.500024$ for the best fit. The Chubukov-Frenkel formula is successful in extracting the superexchange constant, but the line shape given by the theory is too broad.

Canali and Girvin considered the quantum fluctuation effect in the Parkinson's spin wave theory^{25,41} and obtained a line shape (see Fig. ??) which is an improvement but is still a little wider than the Raman data. Numerical calculations of the B_{1g} Raman spectrum of the two-dimensional Heisenberg model were carried out by Sandvik *et al.* within the Loudon-Fleury theory in the spin wave formalism.²⁹ The exact spin wave results give a good fit to the experimental data (see Fig. ??). Based on the above fittings, we also believe that the

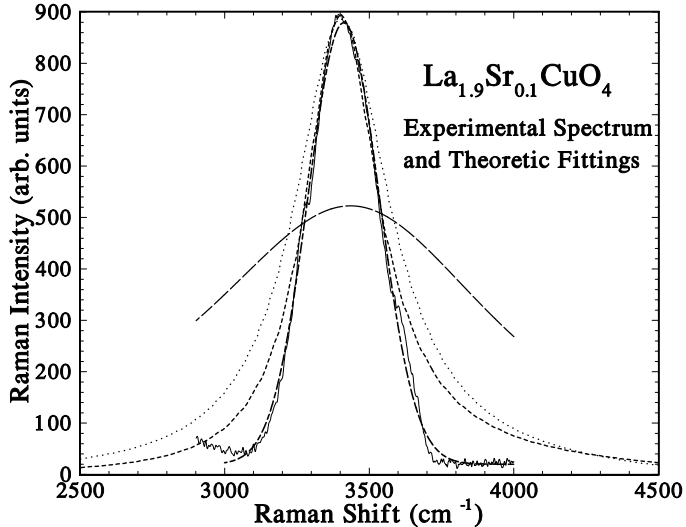


FIG. 4. The Raman spectrum and fits from various theories. The solid curve is the experimental data at 8 K. The long-dash curve is a fit from a formula given by Chubukov and Frenkel.²⁷ The dotted line is a result from Canali and Girvin,²⁵ which includes quantum fluctuation in the ground state. The short-dashed line is an exact spin-wave result by Sandvik *et al.*²⁹ The alt. dashed curve is a Gaussian fit.

main features of the spectrum are due to the Loudon-Fleury mechanism,²⁹ and the quantum fluctuation effect is weak in this system, as we will also show below in calculations of the frequency moment and cumulant. On the other hand, we also tried to fit the peak to a Gaussian or Lorentzian and found that Gaussians give a good fit to the peak. Usually Lorentzians are used to fit Raman data. A good Gaussian fitting indicates a possible multiple-peak structure of the main feature. In Fig. 2 the arrow points to a subsidiary maximum, which could be one of many.

The calculations of the frequency moment and cumulant give us information about the peak symmetry and a parameter-free check on the quantum fluctuation effect. The n th moment of the spectrum^{24,25,29} is defined (at $T=0$) as: $\rho_n = \frac{1}{I_T} \int \omega^n I(\omega) d\omega$, where $I_T = \int I(\omega) d\omega$. The first cumulant $M_1 = \rho_1$, and for $n > 1$,

$$(M_n)^n = \frac{1}{I_T} \int (\omega - \rho_1)^n I(\omega) d\omega \quad (3)$$

The first cumulant, M_1 , gives the mean position of the Raman intensity, while the second and third cumulants M_2 and M_3 measure the width and the asymmetry of the line shape. Using the Raman data at 8 K, We obtain $M_1=3411 \pm 4$ cm⁻¹, $M_2=121 \pm 3$ cm⁻¹, and $M_3=62 \pm 5$ cm⁻¹, where the uncertainties reflect the difference of calculations with and without background. Therefore $M_2/M_1=0.035$, and $M_3/M_1=0.018$. These values differ considerably from the values ($M_2/M_1=0.23$, and $M_3/M_1=0.26$)^{24,25} which were obtained including quantum fluctuation effect, and are also three times smaller

than the Parkinson's results for $S=1/2$ ($M_2/M_1=0.107$, and $M_3/M_1=0.056$). The smaller M_2 and M_3 values tell us that the line width is small, and that the line shape is almost symmetrical, and therefore the quantum fluctuation effect is very weak in $\text{La}_{1.9}\text{Sr}_{0.1}\text{CuO}_4$.

Now we try to explain the appearance of the Raman-forbidden lines in La_2CuO_4 . Motivated by the facts that the unexpected Raman lines from $\text{YBa}_2\text{Cu}_3\text{O}_6$ were explained by Heyen, Kircher and Cardona³⁹ using a Fröhlich interaction, and that the forbidden Raman peaks in La_2CuO_4 have the same values as the infrared LO phonons, we also try to assign the Fröhlich interaction as the cause of the additional lines in La_2CuO_4 . The forbidden first-order intraband Fröhlich interaction results from an expansion in the components of q of the matrix element describing the long-range contribution to the electron-phonon Hamiltonian.⁵⁴ The Fröhlich Hamiltonian H_F is given by:

$$H_F = \frac{C_F}{|q|} (e^{i\frac{\mu}{m_e}q \cdot r} - e^{i\frac{\mu}{m_h}q \cdot r}) \quad (4)$$

where C_F is the Fröhlich coupling constant; m_e and m_h are the effective band masses of the electron and hole, respectively, μ is the reduced mass, and r is the coordinate for the relative motion of the electron and hole. Upon expansion in q of the exponential in Eq. 4, the third term, proportional to $|q|$, is responsible for the so-called forbidden LO-scattering. Because it is zero for $q=0$, this term is often referred as “forbidden”. Under resonance conditions, it can produce higher scattering efficiencies than the “allowed” scattering, in the case of LO-phonons in materials with inversion symmetry.

Several facts support the Fröhlich model: (i) the presence of a center of inversion in La_2CuO_4 ; (ii) the “forbidden” Raman peaks are stronger than the allowed ones and therefore greatly enhanced; (iii) there is a strong electron-phonon interaction in La_2CuO_4 because the phonon at 693 cm⁻¹, the highest frequency vibration, has been found to have strong electron-phonon coupling;^{37,55,56} (iv) the strong Raman peaks involve the scattering from Brillouin zone-middle phonons. Thus the “forbidden” Raman lines come from phonons with q not equal to zero; (v) The last one is the most important fact. As we can see from Table I, the Raman frequencies are almost the same as the LO phonons calculated recently by Kovel *et al.* in Ref. 49. The Raman frequencies 169, 461, 567 and 693 cm⁻¹ are very close to the LO phonon energies of 168, 460, 566 and 692 cm⁻¹, respectively.

V. SUMMARY

In summary, we have observed strong two-magnon Raman scattering in $\text{La}_{2-x}\text{Sr}_x\text{CuO}_4$ ($x=0.1$) as the spin

phase is ordered below 37 K. The line shape and the temperature dependence of the magnetic scattering are totally different from that observed in the parent compound La_2CuO_4 . The two-magnon Raman intensity increases with decreasing temperatures. The temperature dependence of the peak frequency has a two-dimension behavior. The line shape is fitted within the traditional Loudon-Fleury Raman theory and the superexchange constant has been found to be 1052 cm^{-1} . No quantum fluctuation effect has been observed in the system. The Raman scattering in La_2CuO_4 has been found to be very unusual under the excitation of an infrared laser. We have also observed, in the Raman spectrum of La_2CuO_4 , seven usually-Raman-inactive LO phonons which possibly become Raman active via a Fröhlich interaction.

VI. ACKNOWLEDGEMENTS

The work at UBC was supported by Grant No. 5-85653 from the Natural Sciences and Engineering Research Council (NSERC) of Canada.

-
- ¹ A. R. Moodenbaugh *et al.*, Phys. Rev. B **38**, 4596 (1988).
² J. D. Axe *et al.*, Phys. Rev. Lett. **62**, 2751 (1989).
³ G. M. Luke *et al.*, Physica C **185-189**, 1175 (1991).
⁴ I. Watanabe *et al.*, Hyperfine Interact. **86**, 603 (1994).
⁵ G. M. Luke *et al.*, Hyperfine Interact. **105**, 113 (1997).
⁶ K. Kumaga *et al.*, Hyperfine Interact. **86**, 473 (1994); K. Kumaga *et al.*, J. Supercond. **7**, 63 (1994).
⁷ S. Ohsugai *et al.*, J. Phys. Soc. Jap. **63**, 2057 (1994).
⁸ T. Goto *et al.*, J. Phys. Soc. Jap. **66**, 2870 (1997).
⁹ T. Goto *et al.*, J. Phys. soc. Jap. **63**, 3494 (1994).
¹⁰ T. Suzuki *et al.*, Phys. Rev. B **57**, R3229 (1998).
¹¹ Y. Koyama *et al.*, Phys. Rev. B **51**, 9045 (1995).
¹² A. R. Moodenbaugh *et al.*, Phys. Rev. B **58**, 9549 (1998).
¹³ T. Fukase *et al.*, Physica B **165-166**, 1289 (1990).
¹⁴ J. M. Tranquada *et al.*, Nature **375**, 561 (1995).
¹⁵ J. M. Tranquada *et al.*, Phys. Rev. B **54**, 7489 (1996).
¹⁶ B. Nachumi *et al.*, Phys. Rev. B **58**, 8760 (1998).
¹⁷ J.-S. Zhou *et al.*, Phys. Rev. B **56**, 6288 (1997).
¹⁸ J. M. Tranquada *et al.*, Phys. Rev. Lett. **78**, 338 (1997).
¹⁹ G. Blumberg *et al.*, Phys. Rev. Lett. **80**, 564 (1998).
²⁰ K. Yamamoto *et al.*, Phys. Rev. Lett. **80**, 1493 (1998).
²¹ S. Sugai *et al.*, Phys. Rev. B **38**, 6436 (1988).
²² K. B. Lyons *et al.*, Phys. Rev. B **37**, 2353 (1988).
²³ P. E. Sulewski *et al.*, Phys. Rev. B **41**, 225 (1990).
²⁴ R. R. P. Singh *et al.*, Phys. Rev. Lett. **62**, 2736 (1989).
²⁵ C. M. Canali, S. M. Girvin, Phys. Rev. B **45**, 7127 (1992).
²⁶ A. V. Chubukov and D. M. Frenkel, Phys. Rev. Lett. **74**, 3057 (1995).
²⁷ A. V. Chubukov and D. M. Frenkel, Phys. Rev. B **52**, 9760 (1995).
²⁸ D. K. Morr and A. V. Chubukov, Phys. Rev. B **56**, 9134 (1997).
²⁹ A. W. Sandvik *et al.*, Phys. Rev. B **57**, 8478 (1998).
³⁰ P. A. Fleury and R. Loudon, Phys. Rev. **116**, 514 (1968).
³¹ S. M. Hayden *et al.*, Phys. Rev. Lett. **67**, 3622 (1991).
³² P. Bourges *et al.*, Phys. Rev. Lett. **79**, 4906 (1997).
³³ R. Liu *et al.*, J. Phys. Chem. Solids **54**, 1347 (1993).
³⁴ G. Blumberg *et al.*, Phys. Rev. B **53**, R11930 (1996).
³⁵ I. Ohana *et al.*, Phys. Rev. B **40**, 2225 (1989).
³⁶ M. Yoshida *et al.*, Phys. Rev. B **46**, 6505 (1992).
³⁷ W. H. Weber *et al.*, Phys. Rev. B **38**, 917 (1988).
³⁸ S. Sugai, Phys. Rev. B **39**, 4306 (1989).
³⁹ E. T. Heyen, J. Kircher, and M. Cardona, Phys. Rev. B **45**, 3037 (1992).
⁴⁰ G. Wübbeler *et al.*, Phys. Rev. B **54**, 9054 (1996).
⁴¹ J. B. Parkinson, J. Phys. C **2**, 2012 (1969).
⁴² R.R.P. Singh, Phys. Rev. B **39**, 9760 (1989).
⁴³ T. Oguchi, Phys. Rev. **117**, 117 (1960).
⁴⁴ B.I. Kochelaev *et al.*, Phys. Rev. Lett. **79**, 4274 (1997); J. Sichelshmidt, Ph.D. thesis (TH Darmstadt, 1997).
⁴⁵ I. Felner *et al.*, Phys. Rev. B **55**, R3374 (1997); Ch. Niedermayer *et al.*, Phys. Rev. Lett. **80**, 3843 (1998).
⁴⁶ P. A. Fleury and H. J. Guggenheim, Phys. Rev. Lett. **24**, 1346 (1970).
⁴⁷ S. Rosenblum *et al.*, Phys. Rev. B **49**, 4352 (1994).
⁴⁸ S. L. Chaplot *et al.*, Phys. Rev. B **52**, 7230 (1995).
⁴⁹ S. Kovel *et al.*, Phys. Rev. B **51**, 6634 (1995).
⁵⁰ F. Gervais *et al.*, Phys. Rev. B **37**, 9364 (1988).
⁵¹ M. Mostoller *et al.*, Phys. Rev. B **41**, 6488 (1990).
⁵² J. M. Tranquada *et al.*, Phys. Rev. B **52**, 3581 (1995).
⁵³ Y. Murakami *et al.*, Phys. Rev. Lett. **80**, 1932 (1998); B. J. Sternlieb *et al.*, *ibid.* **76**, 2169 (1996).
⁵⁴ M. Cardona, in *Topics in Applied Physics (Light scattering in Solids II)*, edited by M. Cardona and G. Güntherodt (Springer-Verlag, Berlin, 1982), Vol. 50, pp.128.
⁵⁵ W. Weber, Phys. Rev. Lett. **58**, 1371 (1987);
⁵⁶ M. Stavola *et al.*, Phys. Rev. Lett. **58**, 1571 (1987);